Supporting Information

Gold red-ox catalytic cycles for the oxidative coupling of alkynes.

Antonio Leyva-Pérez,[a] Antonio Doménech,[b] Saud I. Al-Resayes,[c] and Avelino Corma.[a,c]*

[a] Instituto de Tecnología Química. Universidad Politécnica de Valencia-Consejo Superior de Investigaciones Científicas. Avda. de los Naranjos s/n, 46022, Valencia, Spain.

[b] Departament de Química Analítica. Universitat de Valencia. Dr. Moliner, 50, 46100 Burjassot (Valencia). Spain.

[c] Chemistry Department, College of Science, King Saud University B.O. BOX.2455 Riyadh 11451 Saudi Arabia.

Corresponding author: acorma@itq.upv.es

Phone: +34963877800; Fax: +349638 77809.

Table of Contents:

General.

Reagents and solvents were obtained from commercial sources and were used without further purification otherwise indicated. Gold (I) complexes $AuPR_3NTf_2$[1,2] were prepared as previously reported, and complex **7** was prepared following a standard procedure for similar compounds.[3] All the products obtained were characterised by GC-MS, ^{1}H- and ^{13}C-NMR, and DEPT. When available, the characterisation given in the literature was used for comparison. Gas chromatographic analyses were performed in an instrument equipped with a 25 m capillary column of 5% phenylmethylsilicone. Dodecane was used as external standard. GC/MS analyses were performed on a spectrometer equipped with the same column as the GC and operated under the same conditions. Column chromatography and TLC were performed over SiO_2. ^{1}H, ^{13}C, DEPT and ^{31}P-NMR measurements were recorded in a 300 MHz instrument using CD_3CN or $CDCl_3$ as solvents, containing TMS as internal standard. IR spectra of the compounds were recorded on a spectrophotometer as self-supported wafers or by impregnating the windows with a dichloromethane solution of the compound and leaving to evaporate before analysis.

Reaction Procedures.

Catalyst screening, selectivity studies, and scope (Table S1 and Scheme 2). The catalyst (0.025 mmol) and, if needed, the oxidant (0.75 mmol) and the base (1 mmol) were placed in a 2 ml vial equipped with a magnetic stir bar. The corresponding solvent (0.5 ml) and phenylacetylene **1** (55 μl, 0.5 mmol) were added, the vial was sealed and the resulting mixture was magnetically stirred for 5-20 h at room temperature. Then, the reaction mixture was poured into diethyl ether (4.5 ml), dodecane (22.4 μl, 0.2 mmol) was added as external standard and 1.5 ml from this mixture was passed through a filter syringe and submitted to GC and GC-MS analysis. For isolation of the product, the whole mixture was submitted to flash column chromatography to give, after removal of the solvents, the corresponding product in pure form. Compound **9** (white solid): R_f (*n*-hexane): 0.51. MS (*m/z*, relative intensity): 230 ($M^{+\cdot}$, 100), 229 (100), 228 (100), 215 (60), 202 (40), 115 (97), 101 (20). IR (υ, cm^{-1}): 2947, 1595, 1455. ^{1}H NMR (δ, ppm; *J*, Hz): 7.51 (aromatic C*H*, 2H, dmult, *J*= 7.8), 7.27 (aromatic C*H*, 2H, td, *J*= 7.7, 1.4), 7.22 (aromatic C*H*, 2H, dmult, *J*= 7.6), 7.14 (aromatic C*H*, 2H, tmult, *J*= 7.5), 2.51 (C*H*$_3$, 6H, s). ^{13}C NMR (δ, ppm): 141.6 (aromatic, 2C), 132.9 (aromatic, 2CH), 129.5

(aromatic, 2CH), 129.1 (aromatic, 2CH), 125.6 (aromatic, 2CH), 121.7 (aromatic, 2C), 81.1 (alkyne, 2C), 77.5 (alkyne, 2C), 20.7 (methyl, $2CH_3$).

In-situ NMR experiments (Figures 1 and S2). The corresponding metal complex **7** (14.3 mg, 0.025 mmol) or *o*-tolylphenylacetylene **8** (6.3 µl, 0.05 mmol), selectfluor (8.8 mg, 0.25 mmol) and, when corresponds, $AuPPh_3NTf_2$ (19.8 mg, 0.025 mmol) or phenylacetylene **1** (2.75 µl, 0.025 mmol) were dissolved in a mixture of CD_3CN:$CDCl_3$ (0.75:0.075 ml) and then H_2O (25 µl) was added. The solution was transferred to a NMR tube containing Na_2CO_3 (2.65-5.3 mg, 0.025-0.05 mmol) if needed. The reaction mixture was followed by ^1H and ^{31}P-NMR spectroscopy at a temperature of 20 ºC.

Kinetics (Figure 2 and S4-S7). $AuPPh_3NTf_2$, selectfluor, and Na_2CO_3 were placed in a 10 ml round-bottomed flask equipped with a magnetic bar. CH_3CN (4 ml) and *o*-tolylphenylacetylene **8** were added, a septum rubber was fitted and the reaction mixture was magnetically stirred in a pre-heated oil bath at 50 ºC for the indicated time. Aliquots (100-200 µl) were periodically taken, poured into dichloromethane (1 ml), filtered and submitted to GC analysis after addition of dodecane (5.6 µl, 0.05 mmol) as external standard.

Cyclic Voltammetry. Electrochemical experiments were performed in 0.1–1.0 mM solutions of the Au(I) complexes in MeCN (Carlo Erba) using Bu_4NPF_6 (Fluka) in concentration 0.10 M as a supporting electrolyte. Measurements were carried out, unless stated, after previous degasification by bubbling Ar during 15 min and maintaining thermostated the cell under an Ar atmosphere at 298±1 K. A conventional three-electrode electrochemical cell was used with a AgCl (3M NaCl)/Ag reference electrode separated from the bulk solution by a salt bridge, a glassy carbon working electrode (BAS MF 2012, geometrical area 0.071 cm^2), and a platinum mesh auxiliary electrode. Cyclic and square wave voltammetry were used as detection modes. Potentials were referred to the Fc^+/Fc couple after adding ferrocene (Fluka) until concentration 0.5 mM.

Characterisation.

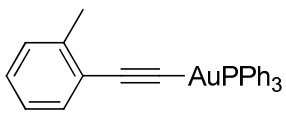

7

Golden-coloured solid. IR (υ, cm^{-1}): 3052, 1479, 1435. ^{1}H NMR (δ, ppm; *J*, Hz): 7.58-7.44 (aromatic C*H*, 18H, mult), 7.39-7.33 (aromatic C*H*, 1H, mult), 7.18-7.01 (aromatic C*H*, 3H, mult), 2.45 (methyl, 3H, mult). ^{13}C NMR (δ, ppm; $J_{C\text{-}P}$, Hz): 139.0 (aromatic, 3C, d, $J_{C\text{-}P}$= 1.6), 133.2 (aromatic, 6CH, d, $J_{C\text{-}P}$= 13.8), 131.5 (aromatic, C), 131.4 (aromatic, CH), 131.0 (aromatic, 3CH), 128.5 (aromatic, 6CH, d, $J_{C\text{-}P}$= 11.5), 128.3 (aromatic, C), 128.2 (aromatic, CH), 125.9 (aromatic, CH), 124.5 (aromatic, CH), 124.2 (alkyne, C, d, $J_{C\text{-}P}$= 1.6), 101.0 (alkyne, C, d, $J_{C\text{-}P}$= 1.6), 19.9 (methyl, CH_3). ^{31}P NMR (δ, ppm): 47.46.

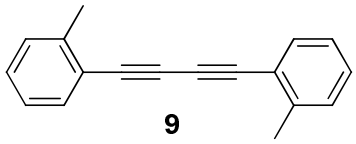

9

White solid. R_f (*n*-hexane): 0.51. MS (*m/z*, relative intensity): 230 ($M^{+\cdot}$, 100), 229 (100), 228 (100), 215 (60), 202 (40), 115 (97), 101 (20). IR (υ, cm^{-1}): 2947, 1595, 1455. ^{1}H NMR (δ, ppm; *J*, Hz): 7.51 (aromatic C*H*, 2H, dmult, *J*= 7.8), 7.27 (aromatic C*H*, 2H, td, *J*= 7.7, 1.4), 7.22 (aromatic C*H*, 2H, dmult, *J*= 7.6), 7.14 (aromatic C*H*, 2H, tmult, *J*= 7.5), 2.51 (C*H*$_3$, 6H, s). ^{13}C NMR (δ, ppm): 141.6 (aromatic, 2C), 132.9 (aromatic, 2CH), 129.5 (aromatic, 2CH), 129.1 (aromatic, 2CH), 125.6 (aromatic, 2CH), 121.7 (aromatic, 2C), 81.1 (alkyne, 2C), 77.5 (alkyne, 2C), 20.7 (methyl, $2CH_3$).

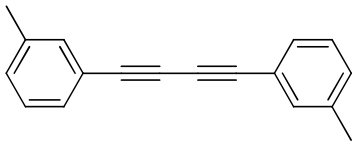

Pale yellow solid. R_f (*n*-hexane): 0.37. MS (*m/z*, relative intensity): 230 ($M^{+\cdot}$, 100), 215 (25), 213 (20), 202 (11). IR (υ, cm^{-1}): 3036, 2916, 1597, 1577, 1481. ^{1}H NMR (δ, ppm; *J*, Hz): 7.34 (aromatic C*H*, 4H, dmult, *J*= 7.4), 7.23 (aromatic C*H*, 2H, td, *J*= 6.9, 1.1), 7.18 (aromatic C*H*, 2H, dmult, *J*= 7.6), 2.34 (C*H*$_3$, 6H, d, *J*= 0.6). ^{13}C NMR (δ, ppm): 138.1 (aromatic, 2C), 133.0 (aromatic, 2CH), 130.1 (aromatic, 2CH), 129.6 (aromatic, 2CH), 128.3 (aromatic, 2CH), 121.6 (aromatic, 2C), 81.6 (alkyne, 2C), 73.6 (alkyne, 2C), 21.2 (methyl, $2CH_3$).

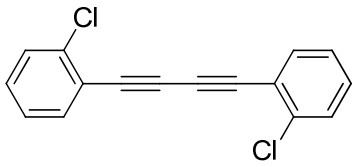

White solid. R_f (*n*-hexane): 0.41. MS (*m/z*, relative intensity): 274 (32), 273 (33), 272 (100), 271 (55), 270 ($M^{+\cdot}$, 100), 234 (11), 200 (100). IR (υ, cm^{-1}): 2971, 2925, 1466, 1435. ^{1}H NMR (δ, ppm; *J*, Hz): 7.58 (aromatic C*H*, 2H, ddd, *J*= 7.7, 1.8, 0.4), 7.42 (aromatic C*H*, 2H, ddd, *J*= 7.9, 1.5, 0.4), 7.31 (aromatic C*H*, 2H, td, *J*= 7.9, 1.9), 7.24 (aromatic C*H*, 2H, td, *J*= 7.6, 1.7). ^{13}C NMR (δ, ppm): 137.0 (aromatic, 2C), 134.4 (aromatic, 2CH), 130.3 (aromatic, 2CH), 129.4 (aromatic, 2CH), 126.5 (aromatic, 2CH), 121.8 (aromatic, 2C), 79.4 (alkyne, 2C), 78.4 (alkyne, 2C).

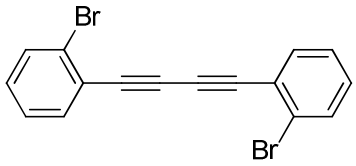

Pale yellow solid. R_f (*n*-hexane): 0.39. MS (*m/z*, relative intensity): 363 (15), 362 (89), 361 (32), 360 (100), 359 (17), 358 ($M^{+\cdot}$, 98), 200 (100). IR (υ, cm^{-1}): 2925, 1431. ^{1}H NMR (δ, ppm; *J*, Hz): 7.61 (aromatic C*H*, 2H, dd, *J*= 8.2, 1.5), 7.58 (aromatic C*H*, 2H, dd, *J*= 7.8, 1.9), 7.30 (aromatic C*H*, 2H, td, *J*= 7.5, 1.4), 7.23 (aromatic C*H*, 2H, td, *J*= 7.6, 1.9). ^{13}C NMR (δ, ppm): 134.5 (aromatic, 2CH), 132.6 (aromatic, 2CH), 130.4 (aromatic, 2CH), 127.1 (aromatic, 2CH), 126.2 (aromatic, 2C), 124.1 (aromatic, 2C), 81.1 (alkyne, 2C), 77.9 (alkyne, 2C).

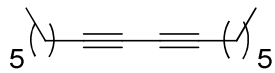

R_f (*n*-hexane): 0.58. MS (*m/z*, relative intensity): 218 ($M^{+\cdot}$, <5), 189 (21), 91 (100). IR (υ, cm^{-1}): 2957, 2932, 2872, 2859, 1466, 1457. ^{1}H NMR (δ, ppm; *J*, Hz): 2.24 (CH_2, 4H, t, *J*= 7.0), 1.51 (CH_2, 4H, quint, *J*= 7.0), 1.43-1.23 (CH_2, 12H, mult), 0.88 (CH_3, 6H, t, *J*= 6.8). ^{13}C NMR (δ, ppm): 77.5 (alkyne, 2C), 65.2 (alkyne, 2C), 31.3 ($2CH_2$), 28.5 ($2CH_2$), 28.3 ($2CH_2$), 22.5 ($2CH_2$), 19.2 ($2CH_2$), 14.1 (methyl, $2CH_3$).

References.

[1] Leyva, A.; Corma, A. *J. Org. Chem.* **2009**, *74*, 2067.

[2] Corma, A.; Ruiz, V.; Leyva-Pérez, A.; Sabater, M. J. *Adv. Synth. Catal.* **2010**, *352*, 1701.

[3] Cross, R. J.; Davidson, M. F. *J. Chem. Soc. Dalton Trans.* **1986**, 411.

Schemes.

Scheme S1. Oxidation of the gold catalyst with selectfluor and non reactivity of the organogold(III) intermediate.

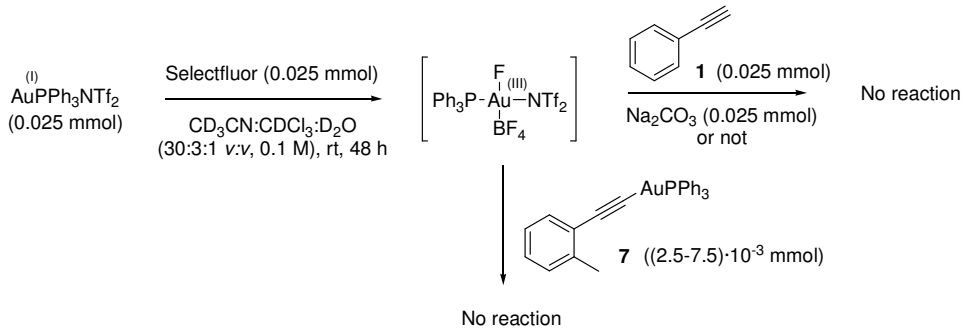

Scheme S2. Kinetic equation calculation for the gold-catalyzed homocoupling of alkynes.

If we define the gold-catalyzed oxidative homocoupling of *ortho*-tolylacetylene **8** as follows,

$$2\cdot\mathbf{8} + \text{Select-F} + 2\text{B} \underset{k_{-1}}{\overset{\text{Cat}\ k_1}{\rightleftharpoons}} \mathbf{9} + \text{Select-noF} + 2\cdot\text{BH} \qquad \text{(Eq. 1)}$$

(Cat: $AuPPh_3NTf_2$, Select-F: Selectfluor, B= Na_2CO_3)

Developing the different individual steps of Equation 1:

$$2\ \text{X} \left(\mathbf{8} + \text{Cat} \underset{k_{-2}}{\overset{k_2}{\rightleftharpoons}} \text{Cat-}\mathbf{8} \right) \qquad \text{(Eq. 3)}$$

$$2\ \text{X} \left(\text{Cat-}\mathbf{8} + \text{B} \underset{k_{-3}}{\overset{k_3}{\rightleftharpoons}} \mathbf{7} + \text{BH} \right) \qquad \text{(Eq. 4)}$$

$$\mathbf{7} + \text{Select-F} \underset{k_{-4}}{\overset{k_4}{\rightleftharpoons}} \mathbf{10} + \text{Select-noF} \qquad \text{(Eq. 5)}$$

$$\mathbf{7} + \mathbf{10} \underset{k_{-5}}{\overset{k_5}{\rightleftharpoons}} \mathbf{9} + 2\cdot\text{Cat} \qquad \text{(Eq. 6)}$$

Sum: Equation 1

In-situ NMR experiments showed that the catalyst $AuPPh_3NTf_2$ (Cat) is immediately transformed to the alkyne adduct (Cat-**8**) under reaction conditions ($k_2 >> k_{-2}$, Equation 3). Similarly, the intermediate **10** was not detected by in-situ NMR experiments and it can be considered that as soon as is formed it reacts with **7** to give **9**. With these two data in hand, as the amount of catalyst is invariant during the process, it can be written:

$$[\text{Cat}]_{\text{total}} = [\text{Cat}] + [\text{Cat-}\mathbf{8}] + [\mathbf{7}] + [\mathbf{10}] \qquad \text{(Eq. 7)}$$

$$\downarrow \quad [\text{Cat}] \approx [\mathbf{10}] \approx 0$$

$$[\text{Cat}]_{\text{total}} = [\text{Cat-}\mathbf{8}] + [\mathbf{7}] \qquad \text{(Eq. 8)}$$

And since Equation 4 is a true equilibrium:

$$Keq_3 = \frac{[\mathbf{7}][BH]}{[\text{Cat-}\mathbf{8}][B]} \longrightarrow [\text{Cat-}\mathbf{8}] = \frac{[\mathbf{7}][BH]}{Keq_3[B]} \quad \text{(Eq. 9)}$$

$$[Cat]_{total} = [\text{Cat-}\mathbf{8}] + [\mathbf{7}] = \frac{[\mathbf{7}][BH]}{Keq'_3[B]} + [\mathbf{7}] = [\mathbf{7}]\left(1 + \frac{[BH]}{Keq'_3[B]}\right) \longrightarrow [\mathbf{7}] = \frac{[Cat]_{total}}{\left(1 + \frac{[BH]}{Keq'_3[B]}\right)} \quad \text{(Eq. 10)}$$

Where $Keq_3' = \sqrt{Keq_3}$, in order to include the double equilibrium in Equation 4. Thus, working out [**7**] in the reaction rate of Equation 5 (remember that [**10**] is very small):

$$r_4 = k_4[\mathbf{7}][\text{Select-F}] - k_{-4}[\mathbf{10}][\text{Select-noF}] = k_4[\mathbf{7}][\text{Select-F}] = \boxed{k_4[Cat]_{total}[\text{Select-F}]\left(\frac{1}{\left(1 + \frac{[BH]}{Keq'_3[B]}\right)}\right)}$$

$[\mathbf{10}] \approx 0$; Eq. 10

(Eq. 2)

Regarding the final reductive homocoupling step (Equation 6), it was checked that the homocoupling products are stable under the reaction conditions and does not go back to the alkyne or to any gold adduct when using gold-catalyzed conditions (see below) thus indicating that $k_5 >> k_{-5}$. Since the lifetime of the gold adduct **10** is very short, this last step can be considered as very fast when compared to the oxidation process (Equation 5).

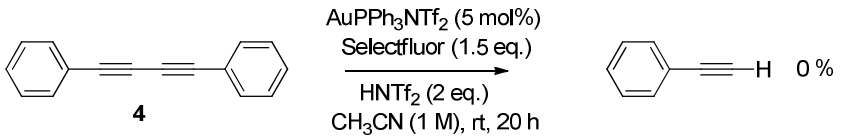

4

Stability of the homocoupling products under acidic gold-catalyzed conditions.

Figures.

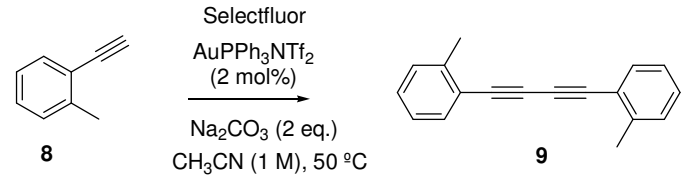

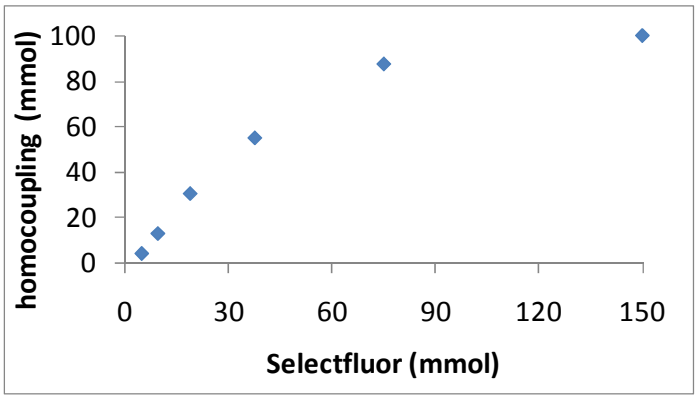

Figure S1. Plot-time yield of **9** for different amounts of selectfluor.

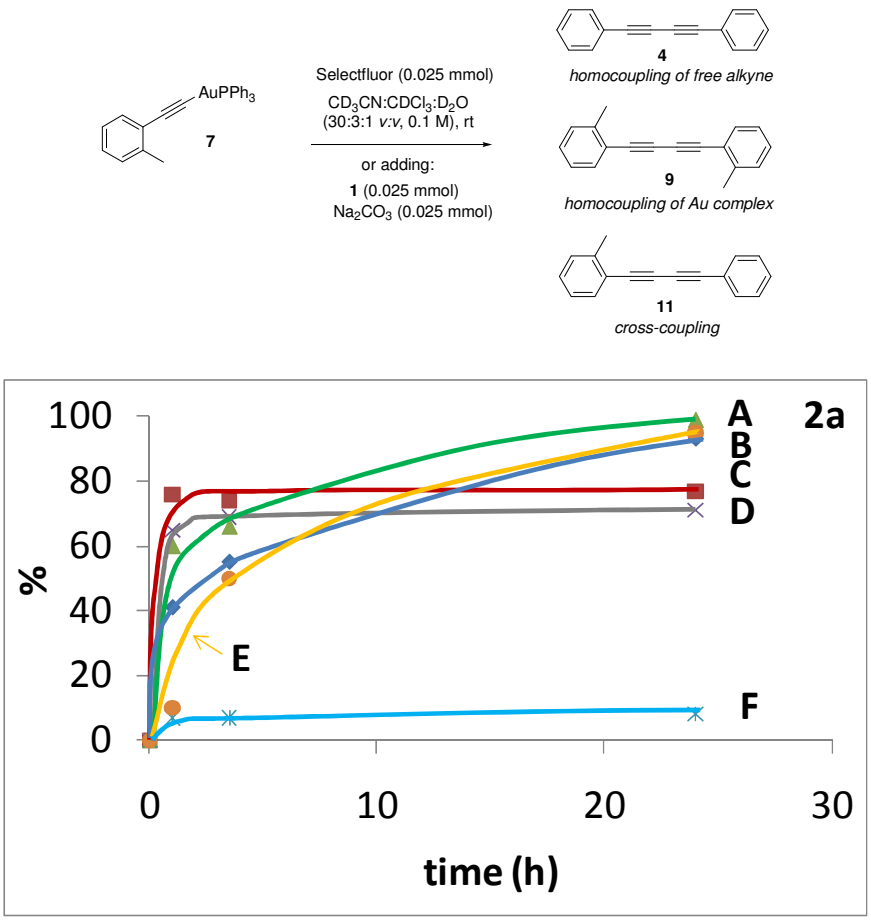

Figure S2. Plot-time yield for: *3a)* conversion of selectfluor for the homocoupling of **7** in the presence (curve A) or in the absence of **1** (curve B), yield of **9** from **7** in the presence (curve D) or in the absence of **1** (curve C), yield of **4** (curve E), and yield of **11** (curve F). The reaction was monitored by *in-situ* ^{1}H and ^{31}P-NMR spectroscopy.

Figure S3. Cyclic voltammograms for: a) 0.2 mM $AuPPh_3NTf_2$ + 0.2 mM selectfluor; b) 0.1 mM $ArCCAuPPh_3$ **7** (Ar= *o*-Tolyl) + 0.2 mM selectfluor; c) 0.2 mM $AuPPh_3NTf_2$ + 0.2 mM selectfluor + 0.2 **7** mM solutions in 0.10 M Bu_4NPF_6/MeCN. Potential scan rate 50 mV/s. Deconvolution has been performed in all voltammograms in order to enhance peak resolution.

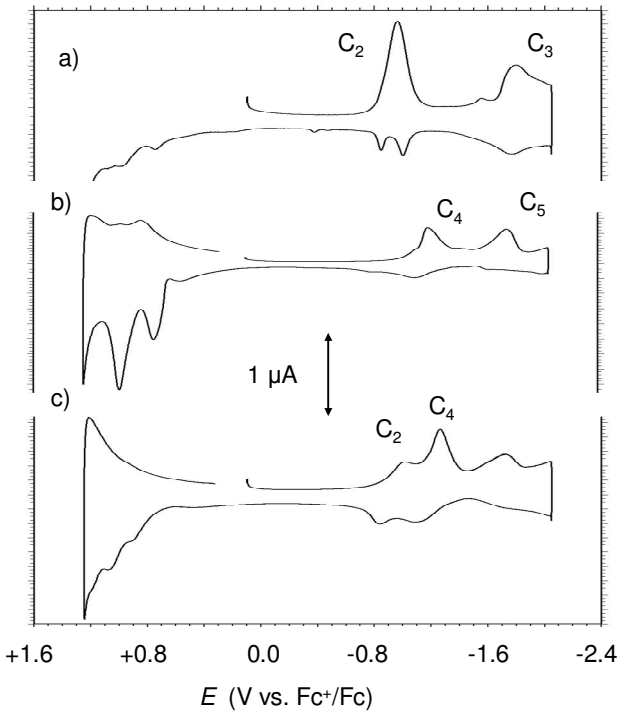

Voltammogram a)

$$PPh_3\text{-}Au(I) + [Fsel](BF_4)_2 \rightarrow PPh_3\text{-}Au(III)F(BF_4) + [sel](BF_4) \quad (1)$$

$$PPh_3\text{-}Au(III)F(BF_4) + 2e^- \rightarrow (1/2)PPh_3\text{-}Au(I)F + (1/2)PPh_3\text{-}Au(I)(BF_4) \quad (2)$$

$$(1/2)PPh_3\text{-}Au(I)F + (1/2)PPh_3\text{-}Au(I)(BF_4) + e^- \rightarrow Au^0 + \text{remainings} \quad (3)$$

Voltammogram b)

$$Ar\text{-}C{\equiv}C\text{-}PPh_3\text{-}Au(I) + [Fsel](BF_4)_2 \rightarrow Ar\text{-}C{\equiv}C\text{-}PPh_3\text{-}Au(III)F(BF_4) + [sel](BF_4) \quad (4)$$

$$Ar\text{-}C{\equiv}C\text{-}PPh_3\text{-}Au(III)F + 2e^- \rightarrow$$

$$\rightarrow (1/2)Ar\text{-}C{\equiv}C\text{-}PPh_3\text{-}Au(I)F + (1/2)Ar\text{-}C{\equiv}C\text{-}PPh_3\text{-}Au(I)(BF_4) \quad (5)$$

$$(1/2)Ar\text{-}C{\equiv}C\text{-}PPh_3\text{-}Au(I)F + (1/2)Ar\text{-}C{\equiv}C\text{-}PPh_3\text{-}Au(I)(BF_4) + e^- \rightarrow Au^0 + \text{remainings} \quad (6)$$

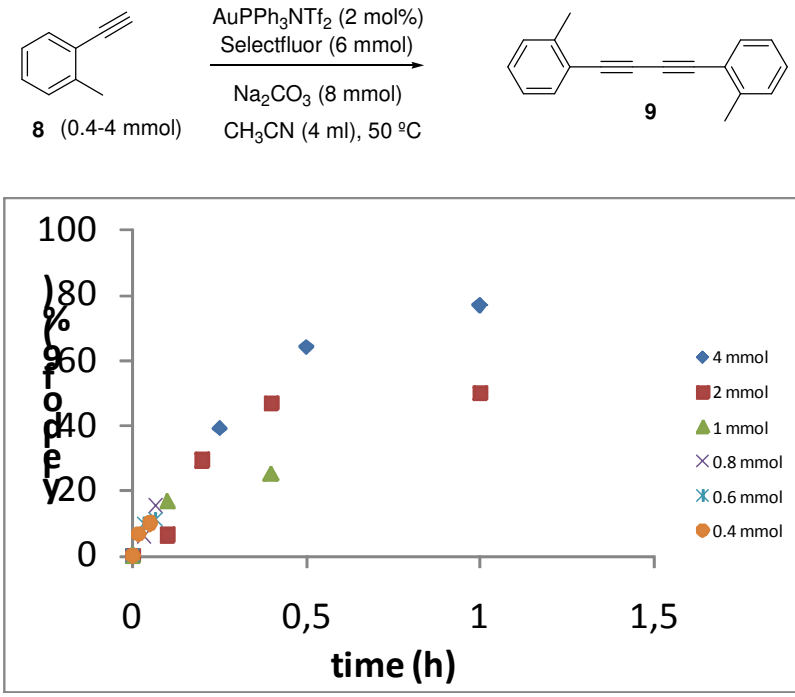

Figure S4. Plot-time yield for different amounts of phenylacetylene **1**.

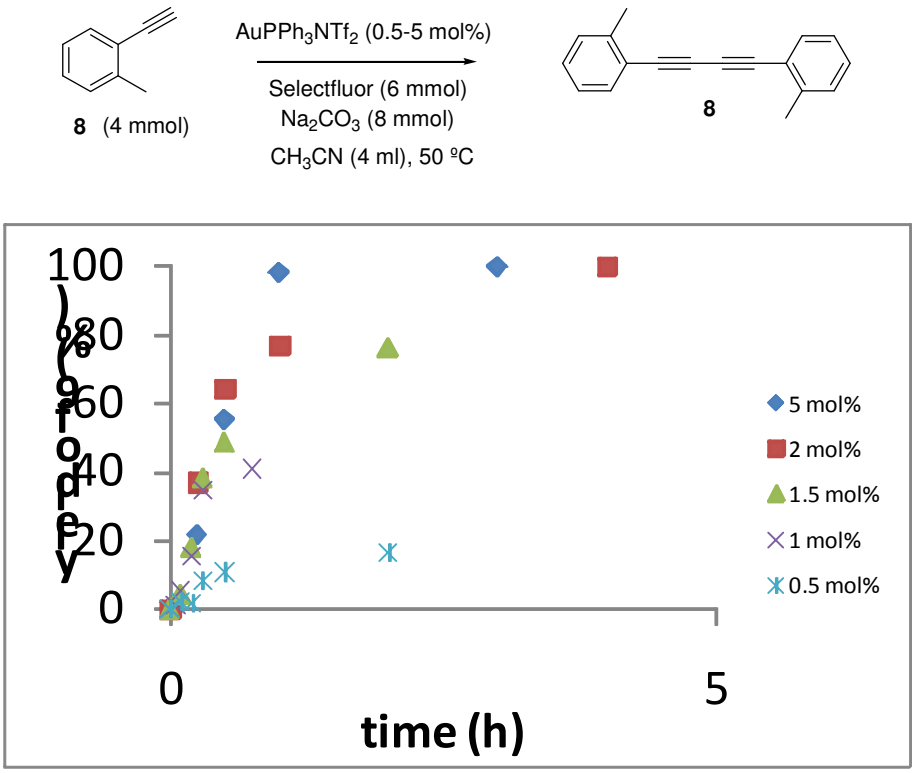

Figure S5. Plot-time yield for different amounts of $AuPPh_3NTf_2$.

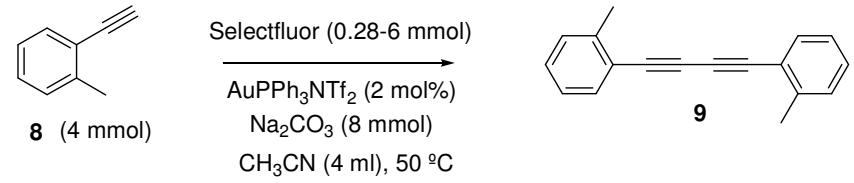

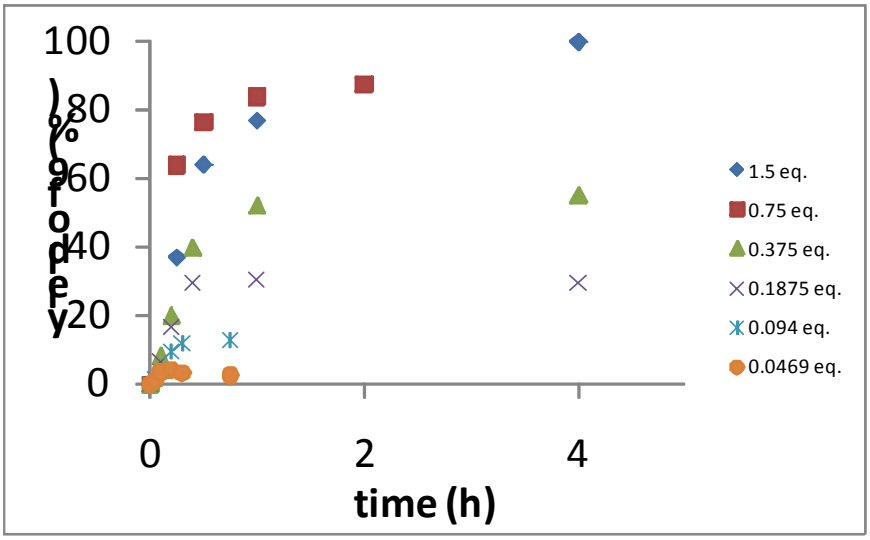

Figure S6. Plot-time yield for different amounts of selectfluor.

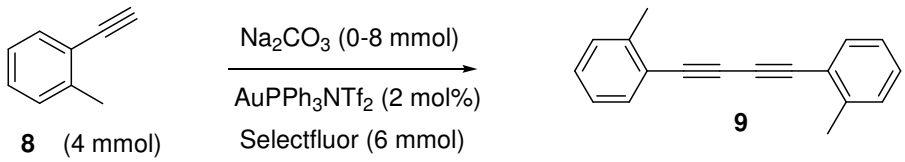

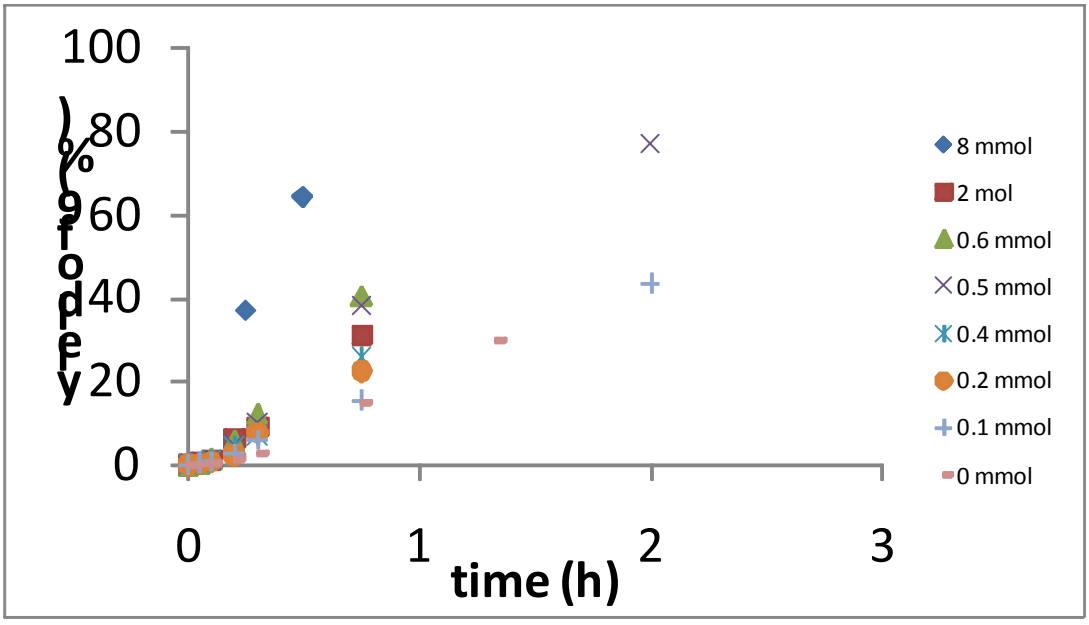

Figure S7. Plot-time yield for different amounts of Na_2CO_3.

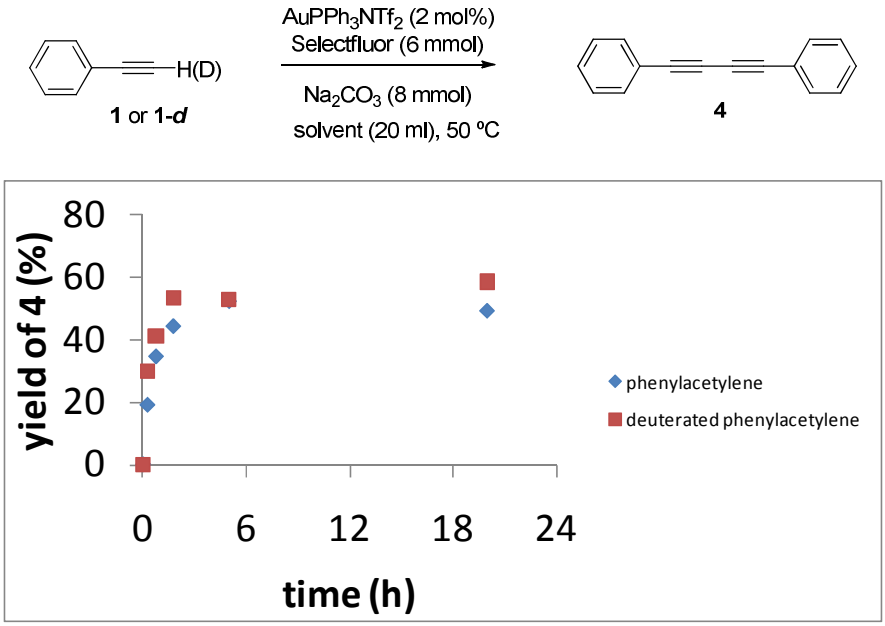

Figure S8. Plot-time yield for kinetic isotopic experiments (1.5 eq. of selectfluor).

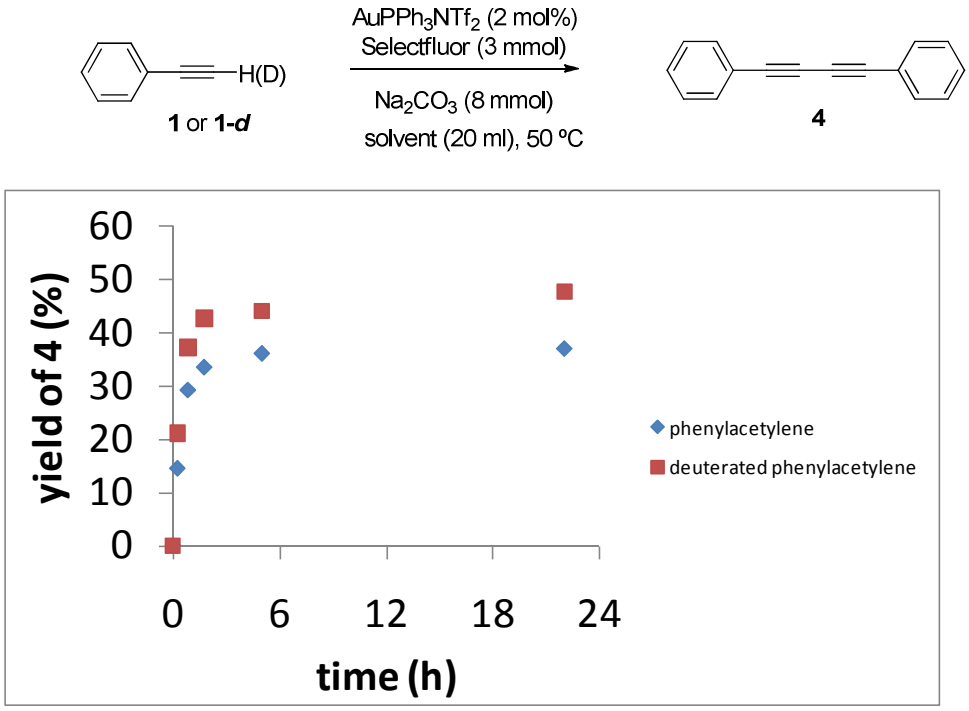

Figure S9. Plot-time yield for kinetic isotopic experiments (0.75 eq. of selectfluor).

Tables.

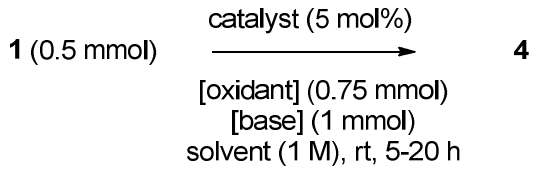

Table S1. Results for the homocoupling of phenylacetylene **1** under different catalyzed conditions.

Run	**Catalyst**	**Oxidant**	**Base**	**Solvent**	**Time (h)**	**Product (%)[a]**
1	$AuPPh_3NTf_2$	none	none	CH_3CN (anhydrous)	5	0
2	AuCl					0
3	$AuCl_3$					0
4	$AuNTf_2$					0[b]
5	$Au(OTf)_3$					0[b]
6	$AgNTf_2$					0
7	$AuPPh_3Cl$					0
8	$AuPPh_3OTf$					0[b]
9	$HAuCl_4{\cdot}3H_2O$					0
10	$Au(NTf_2)_3$					0[b]
11	AuCl	Selectfluor				1
12	$AuPPh_3Cl$					1
13	$AuPPh_3NTf_2$					4
14	$AuNTf_2$					1[b]
15	AuOTf					0[b]
16	$AuPPh_3OTf$					2[b]
17	$AuNTf_2$				20	0[b]
18	$AgNTF_2$					0
19	**$AuPPh_3NTf_2$**					**40**
20				CH_3CN/H_2O (20:1 *v:v*)		10[c]
21		PhI(OOCCF3)2				0[c,d]

22		PhCOOOtBu				0[c]
23		MnO2				0[c]
24		**Selectfluor**		**CH_3CN**		**50 [35][e]**
25				Toluene		0
26				CH_2Cl_2		0
27				1,4-dioxane		0
28				H_2O		0
29			K_3PO_4	CH_3CN		[59] / 24[c]
30			K_2CO_3			31 / 10[c]
31			Cs_2CO_3			14[c]
32			**Na_2CO_3**			**[80] / 21[c]**
33			$KHCO_3$			44 / 20[c,e]
34			$NaHCO_3$			[57] / 34[c,e,f]
35			$Na_3PO4{\cdot}12H_2O$			9[c]
36			KH_2PO_4			10[c,f]
37			$NaH_2PO_4{\cdot}H_2O$			13[c,f]
38			Et_3N			0[c]
39		1-fluoropyridinium sulfate	K_3PO_4			0[c]
40		*N*-fluorobenzenesulfonimide				2[c]
41	$AuSPhosNTf_2$	selectfluor				0[c]
42	$AuDavePhosNTf_2$					1[c]
43	$AuP^tBu_3NTf_2$					0[c]
44	$AgNTf_2$					0[c]
45	**$AuPPh_3NTf_2$**		**Na_2CO_3**			**100**
46	$AuSPhosNTf_2$					18
47	$AuDavePhosNTf_2$					15
48	$AuP^tBu_3NTf_2$					2
49	AuIPrNTf2					0[b]

50	**$AuPPh_3Cl$**					**100**
51	**$AuPPh_3BF_4$**					**74**

[a] GC yield, between brackets isolated yield. [b] Catalyst generated in-situ from the corresponding chloride salt and AgOTf, $AgNTf_2$ or $AgBF_4$. [c] 2 mol% catalyst. [d] 90 % acetophenone product. [e] Full conversion. [f] 2 mmol of base.

NMR spectra.

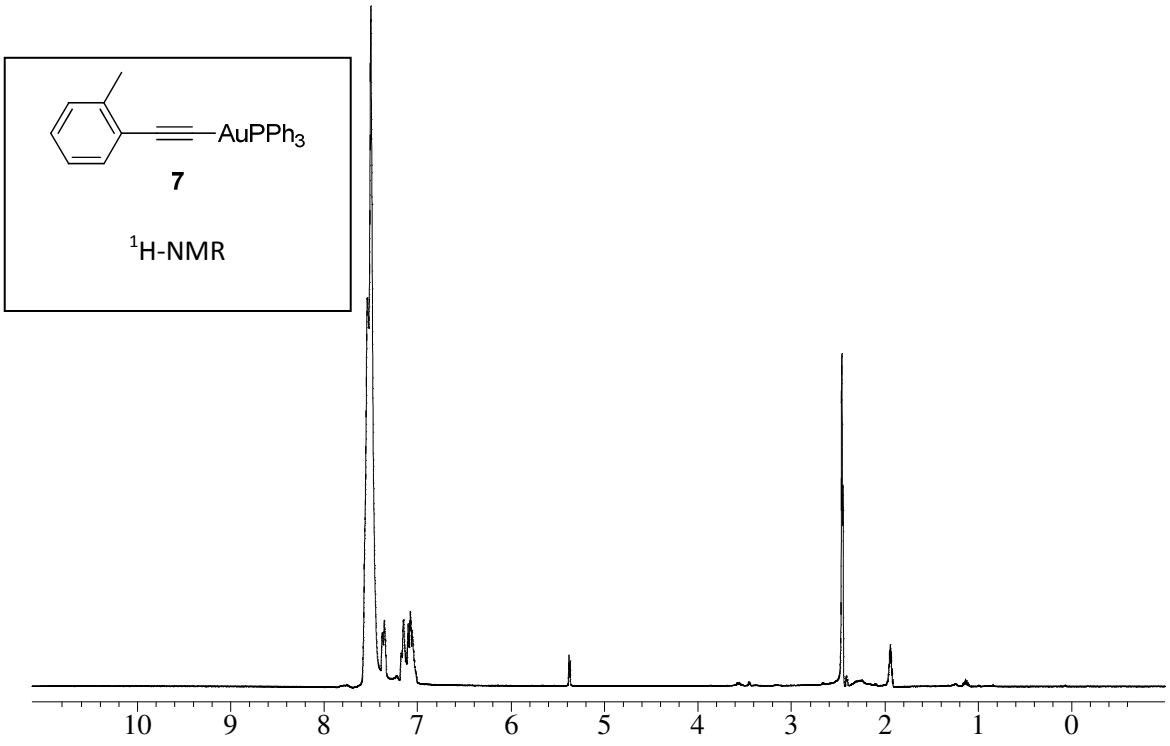
AuPPh3
7
1H-NMR
10
9
8
7
6
5
4
3
2
1
0

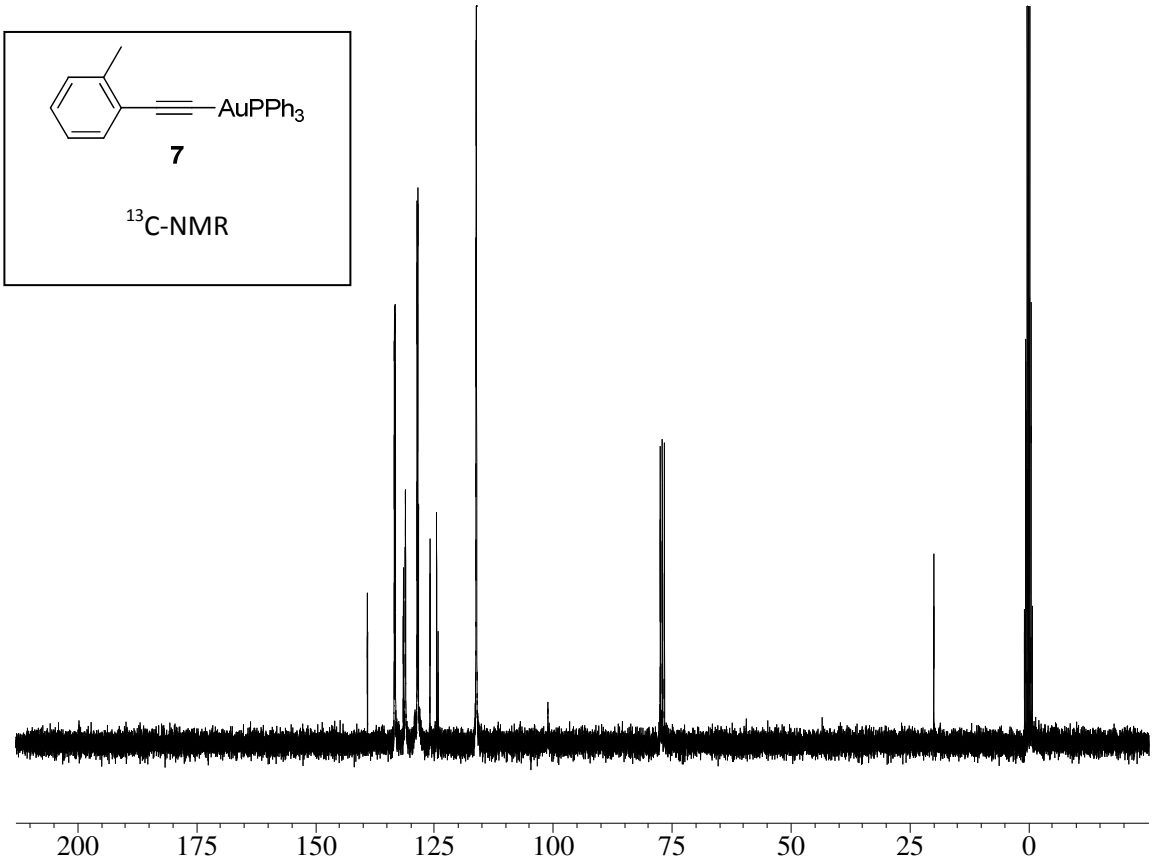
AuPPh3
7
13C-NMR
200
175
150
125
100
75
50
25
0

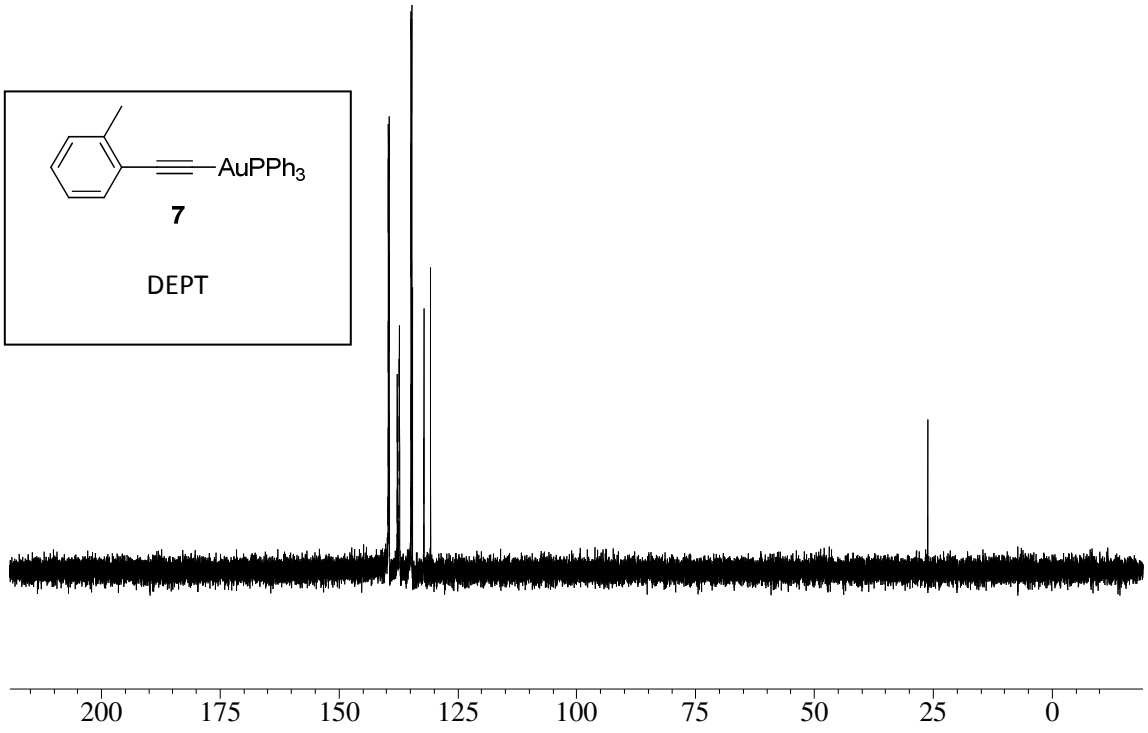
AuPPh3
7
DEPT
200
175
150
125
100
75
50
25
0

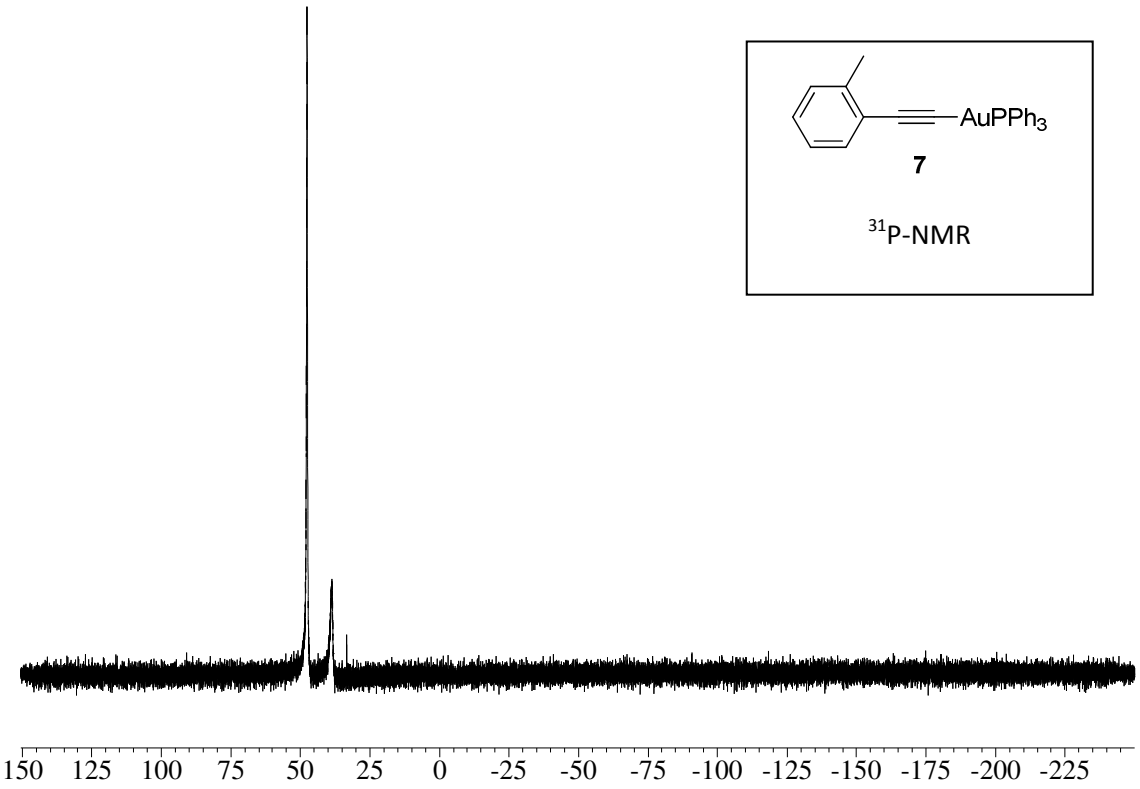
AuPPh3
7
31P-NMR
150
125
100
75
50
25
0
-25
-50
-75
-100
-125
-150
-175
-200
-225

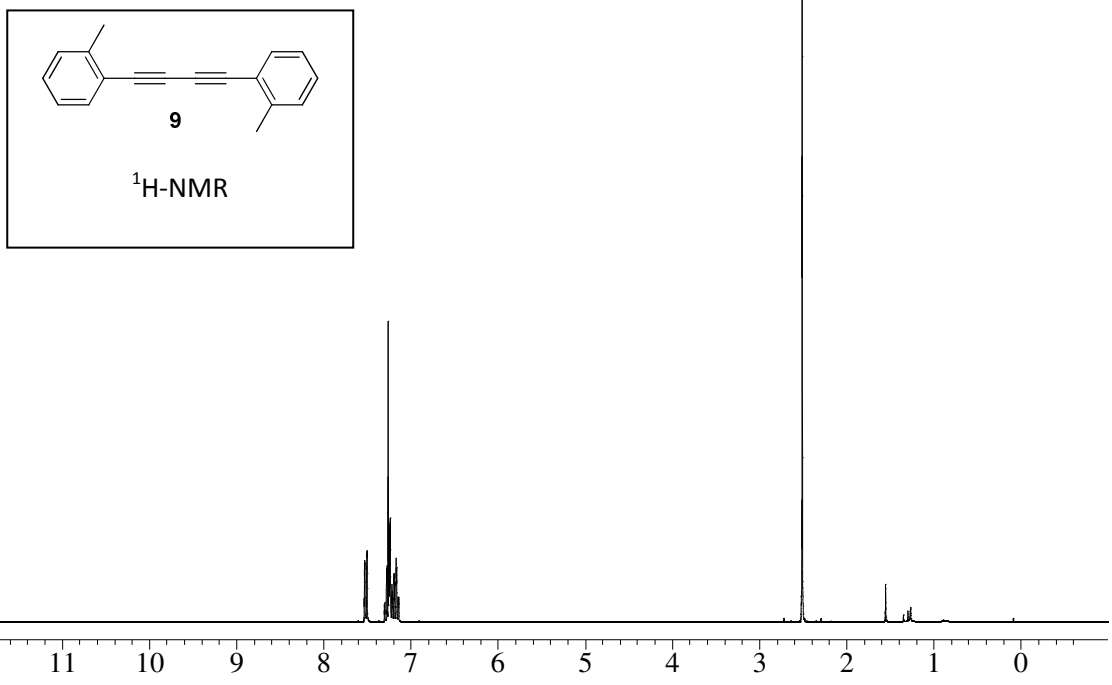
9
1H-NMR
11
10
9
8
7
6
5
4
3
2
1
0

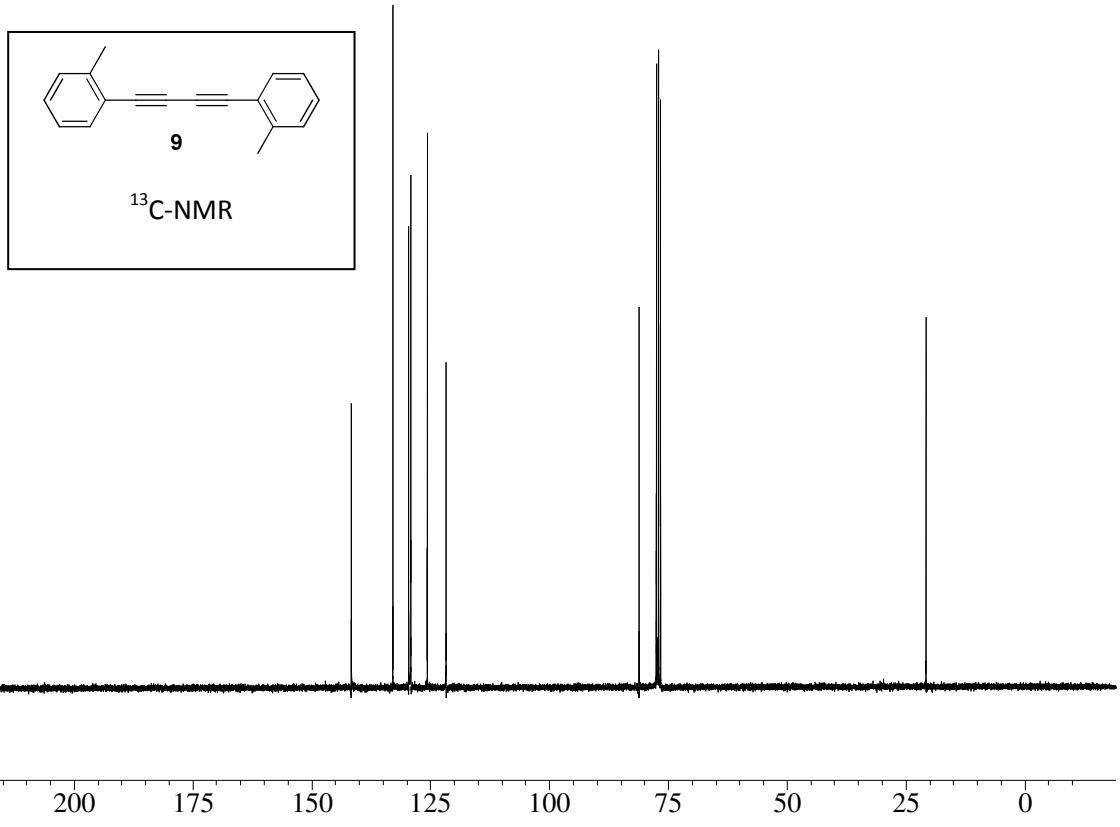
9
13C-NMR
200
175
150
125
100
75
50
25
0

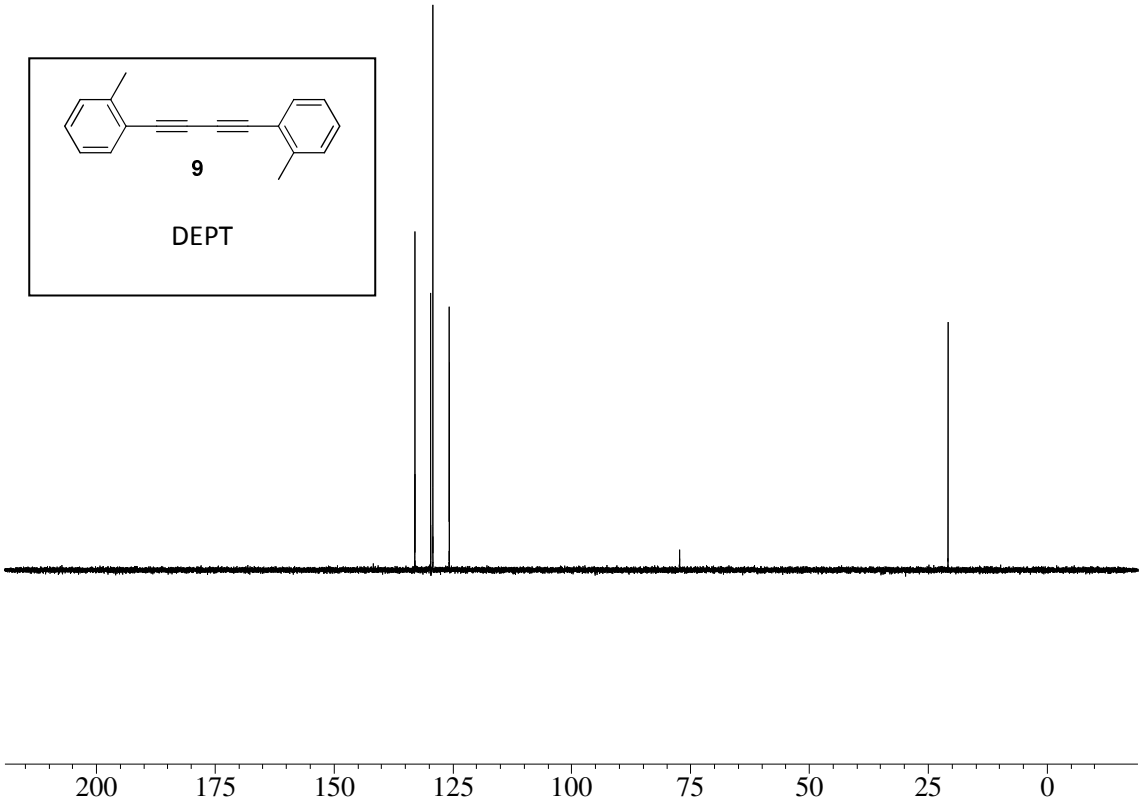
9
DEPT
200
175
150
125
100
75
50
25
0

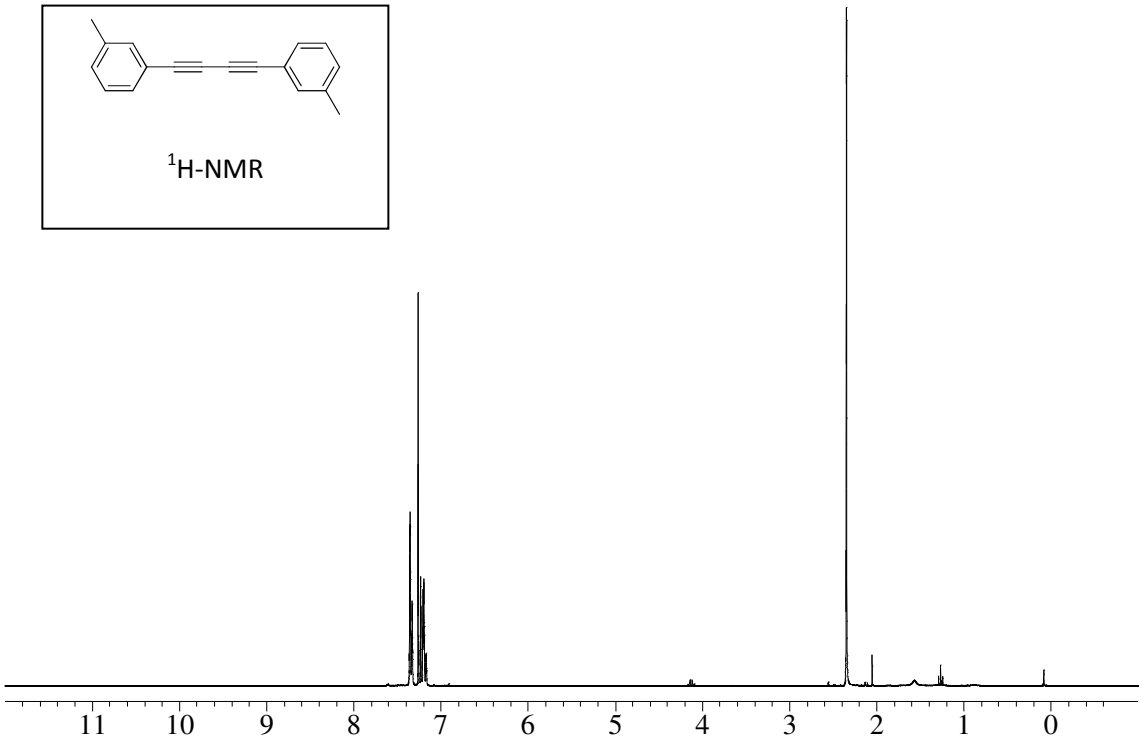
^{1}H-NMR
11
10
9
8
7
6
5
4
3
2
1
0

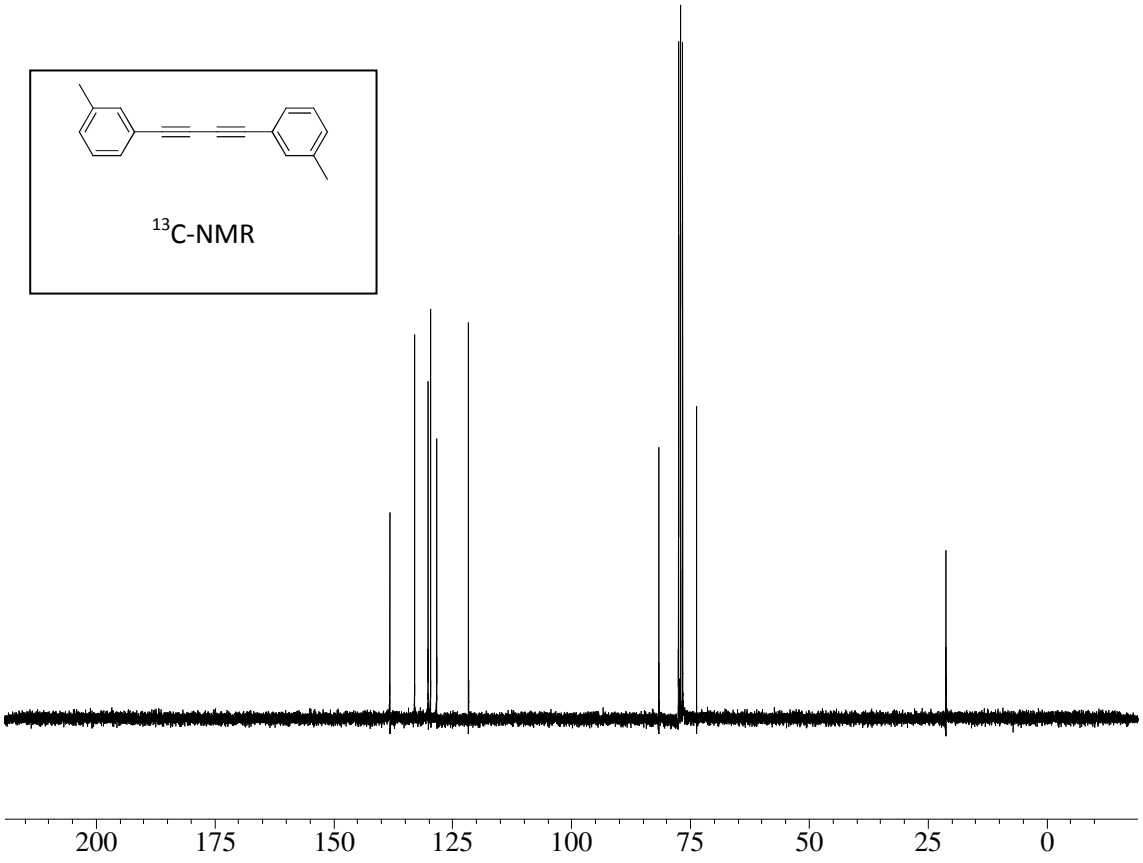
^{13}C-NMR
200
175
150
125
100
75
50
25
0

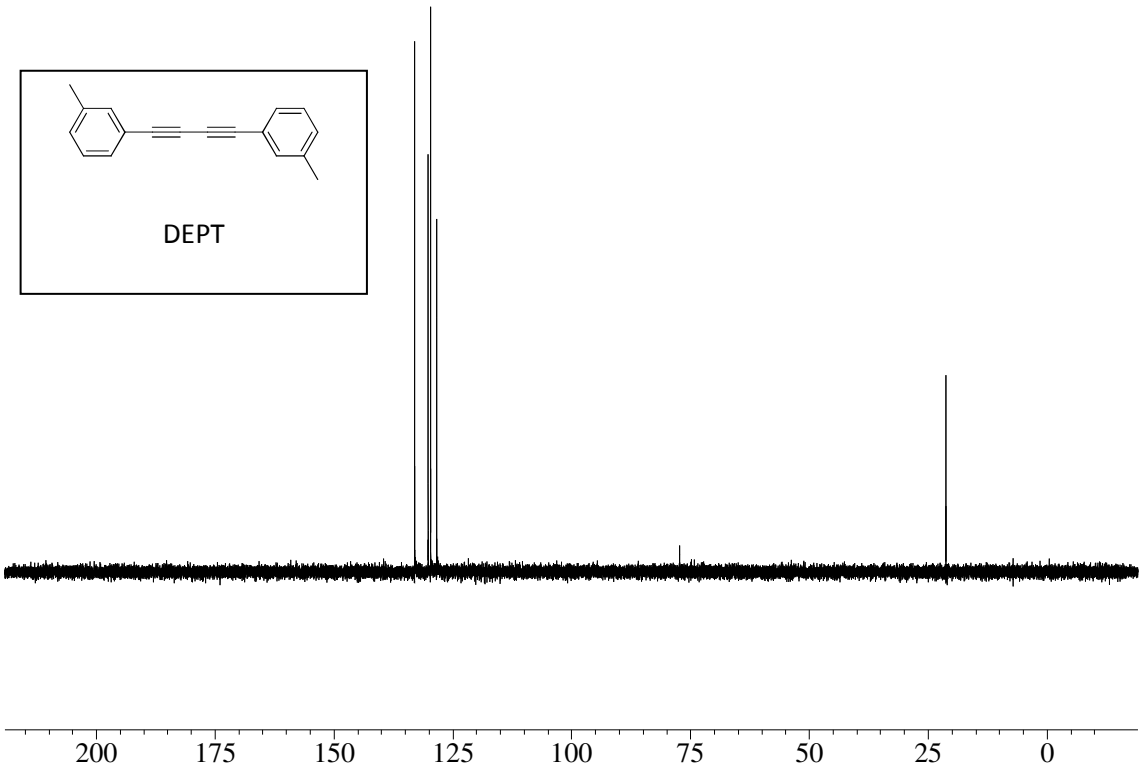
DEPT
200
175
150
125
100
75
50
25
0

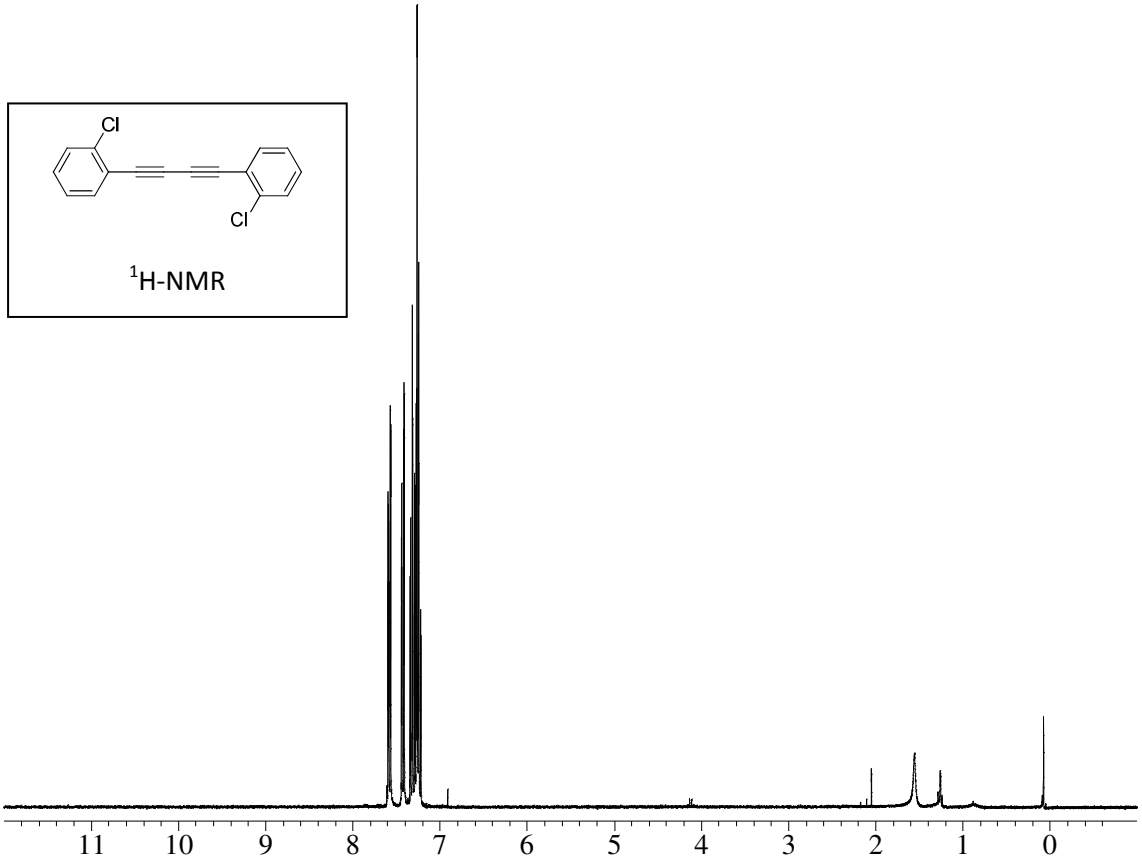
Cl
Cl
1H-NMR
11
10
9
8
7
6
5
4
3
2
1
0

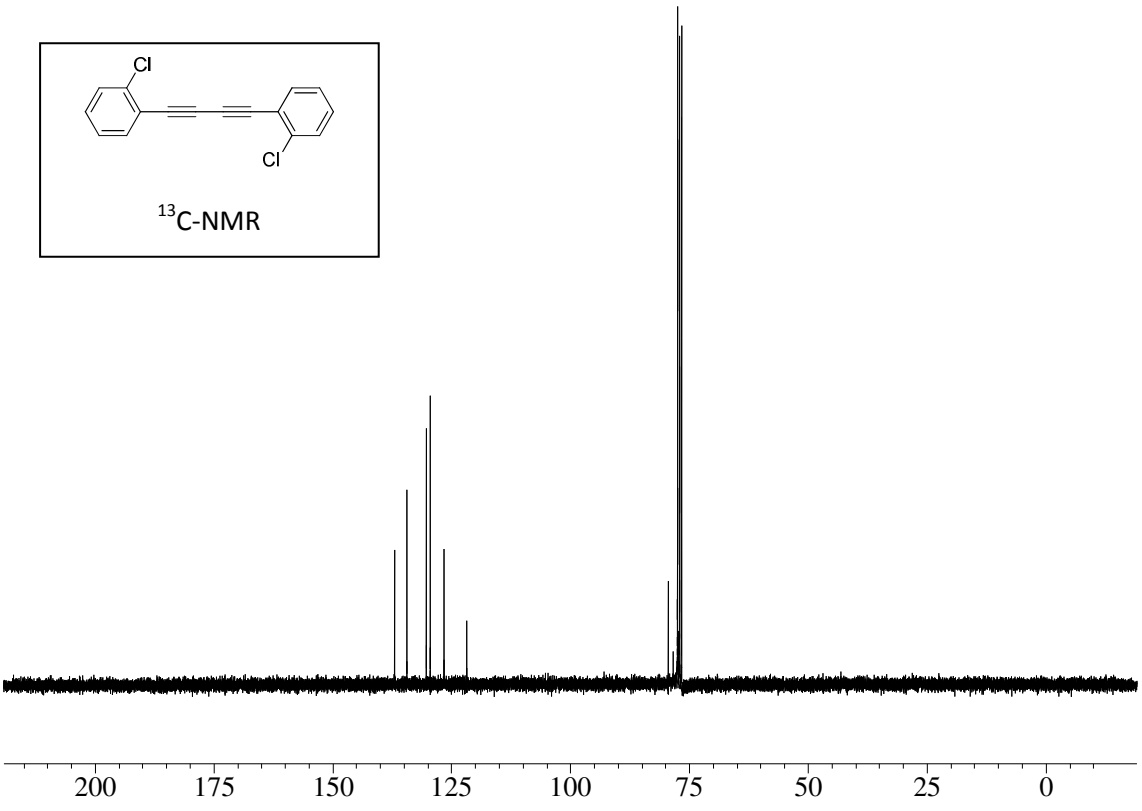
Cl
Cl
13C-NMR
200
175
150
125
100
75
50
25
0

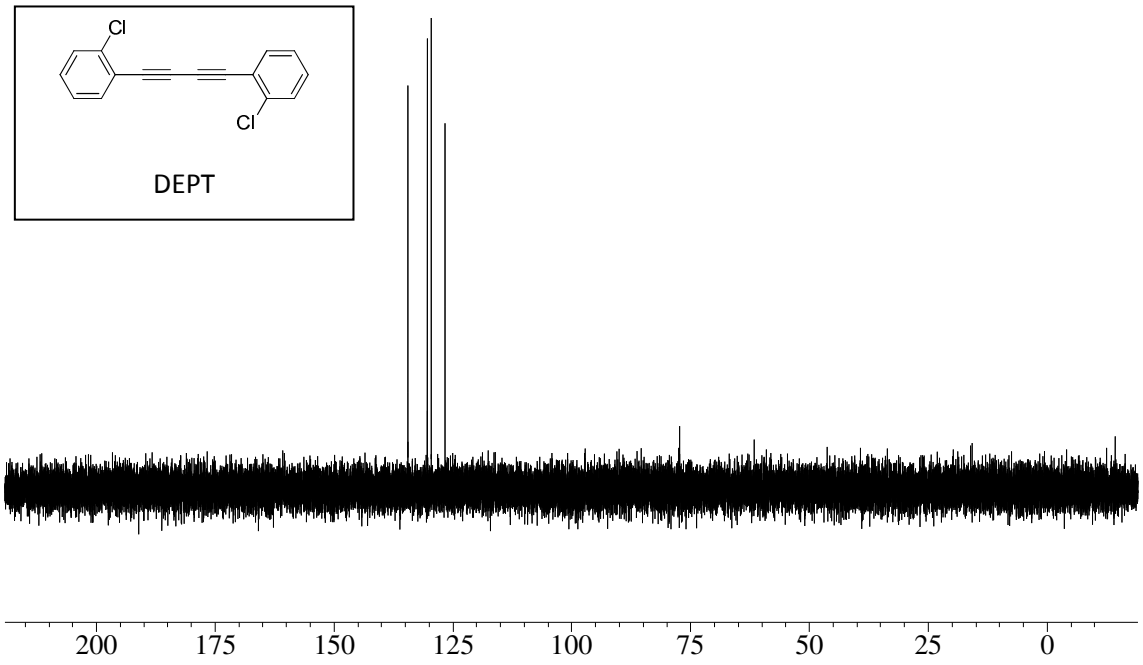
Cl
Cl
DEPT
200
175
150
125
100
75
50
25
0

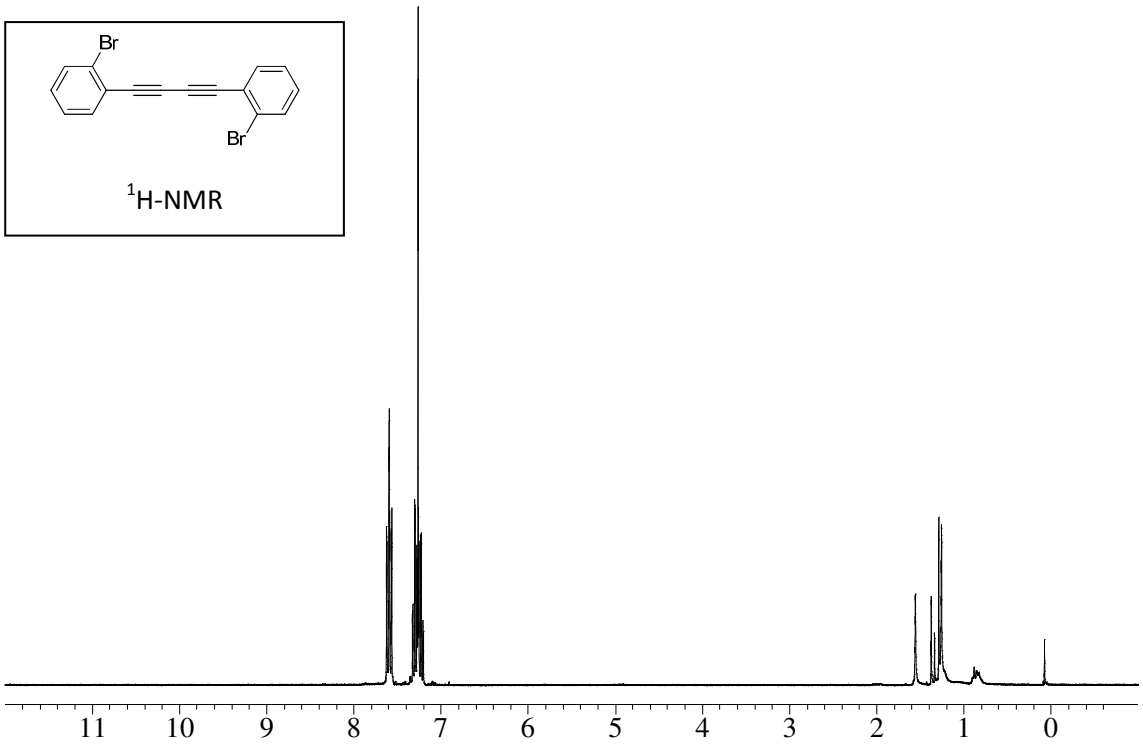
Br
Br
1H-NMR
11
10
9
8
7
6
5
4
3
2
1
0

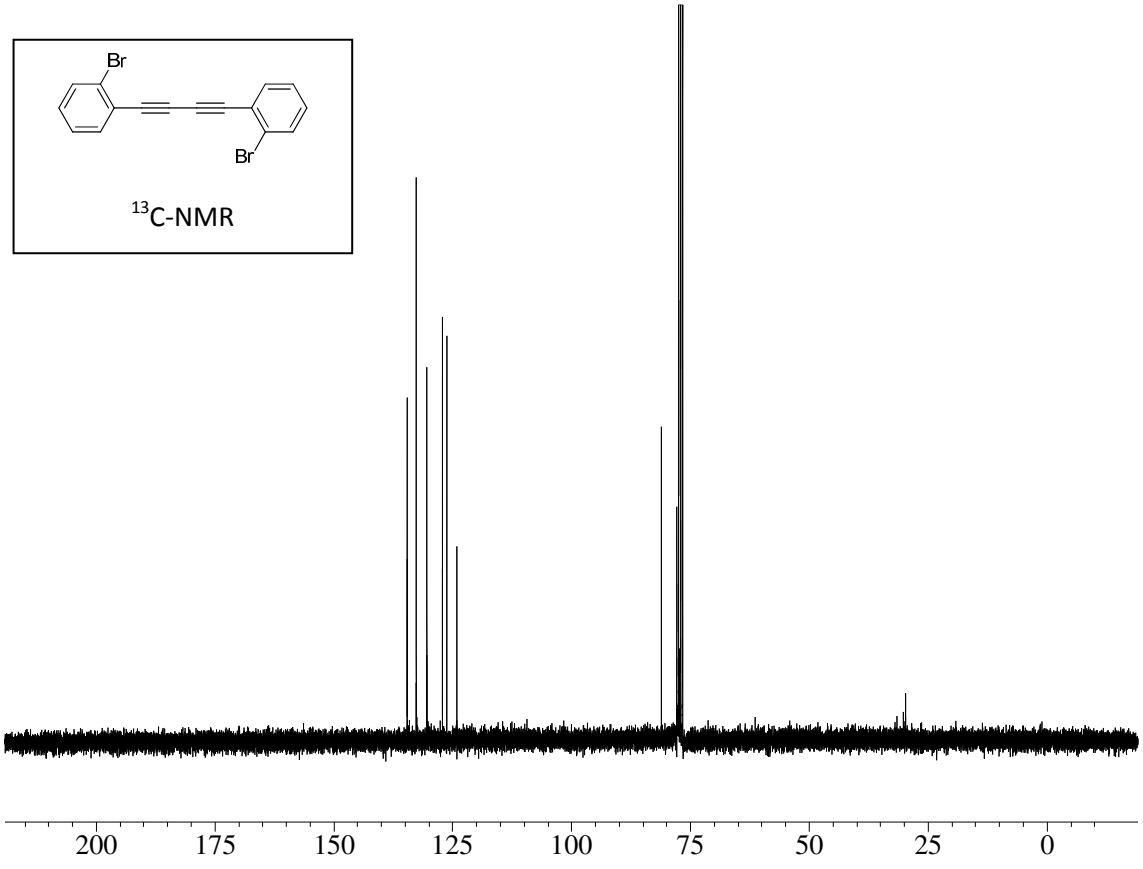
Br
Br
^{13}C-NMR
200
175
150
125
100
75
50
25
0

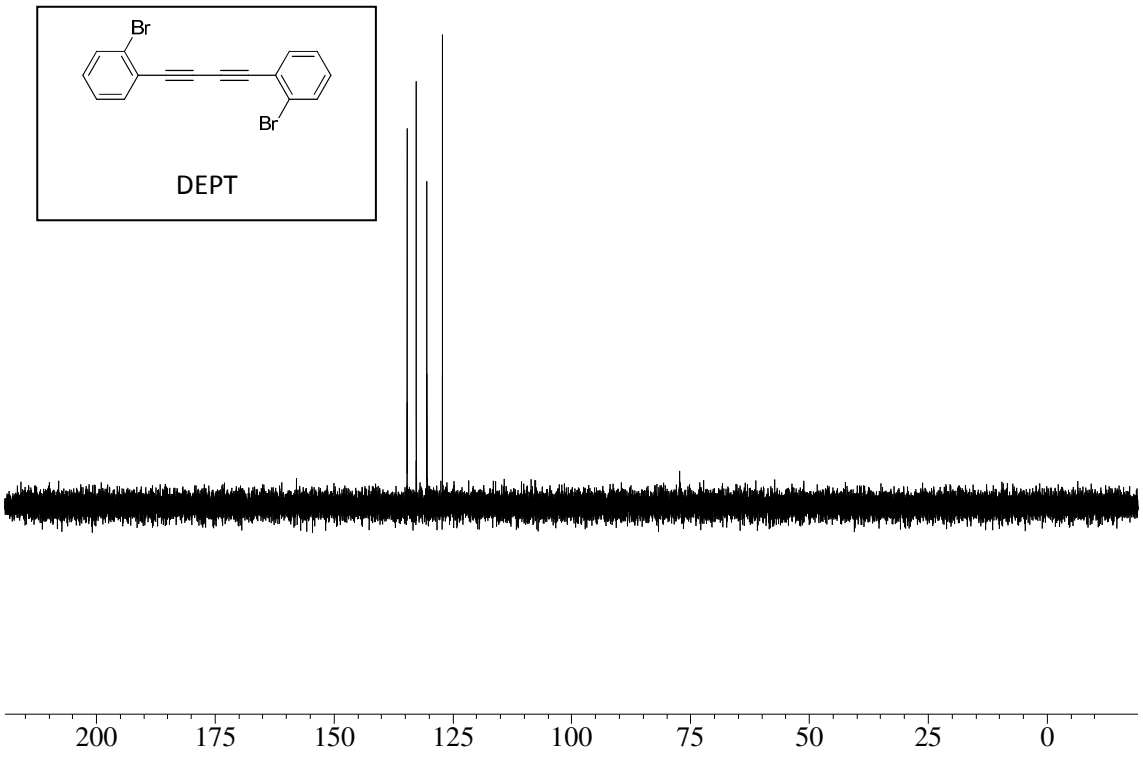
Br
Br
DEPT
200
175
150
125
100
75
50
25
0

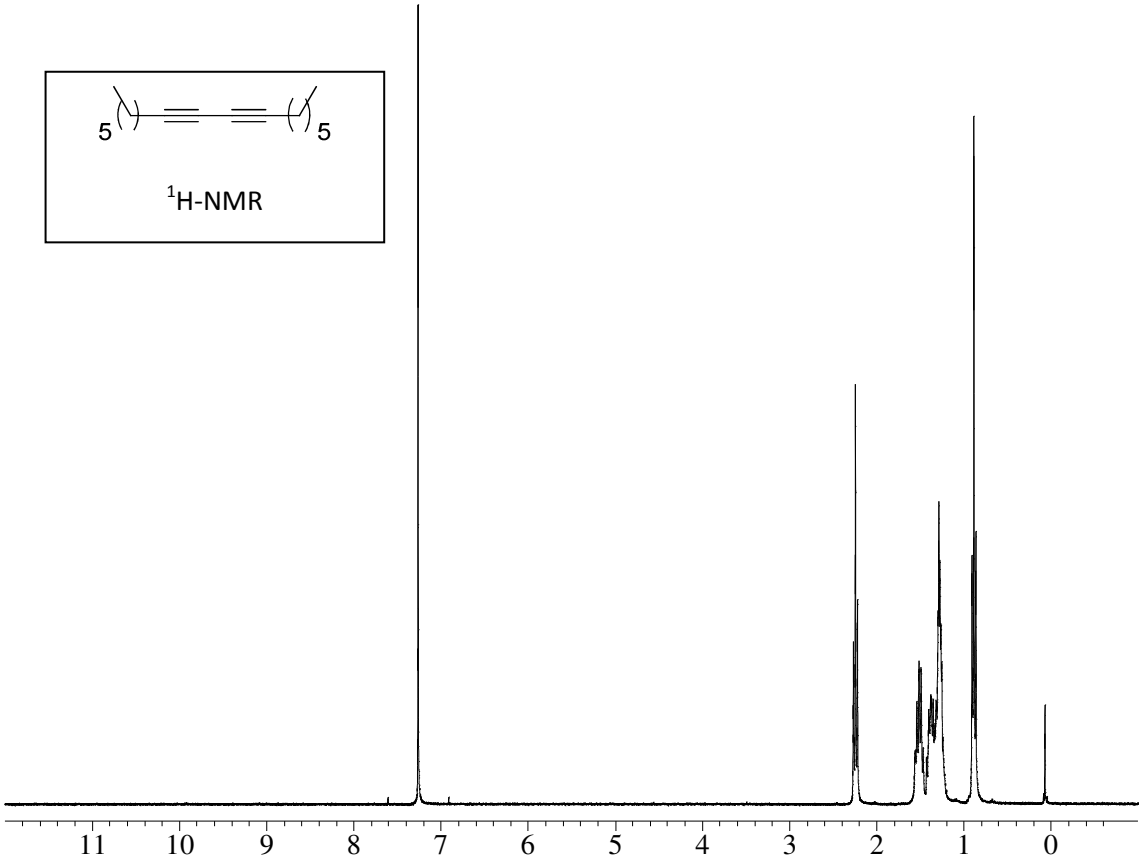
5
5
1H-NMR
11
10
9
8
7
6
5
4
3
2
1
0

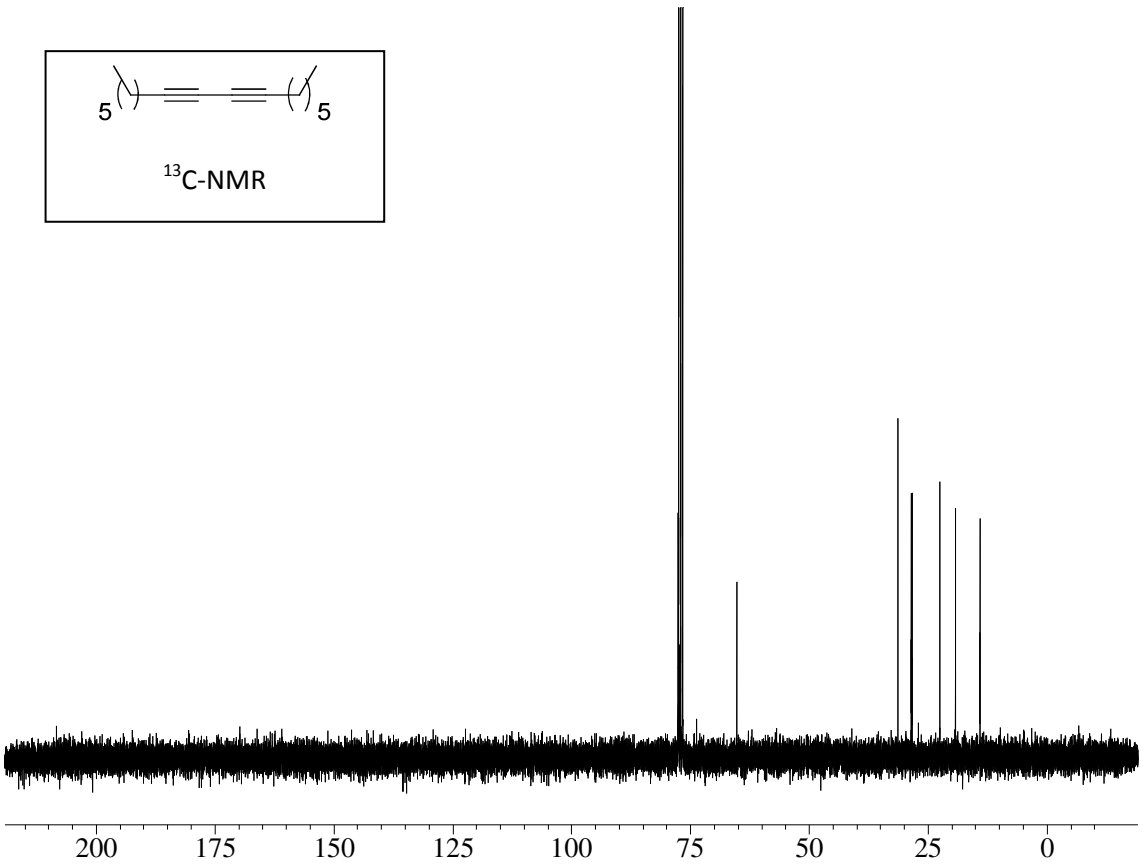
5
5
13C-NMR
200
175
150
125
100
75
50
25
0

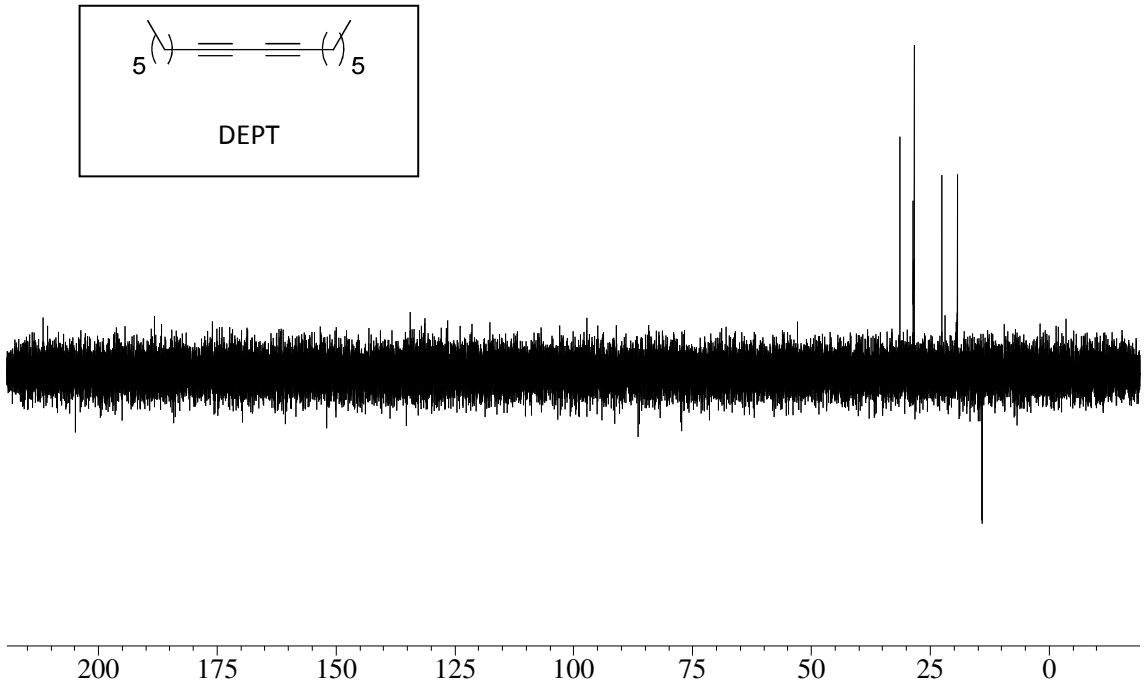
5
5
DEPT
200
175
150
125
100
75
50
25
0